Hindawi Publishing Corporation
International Journal of Antennas and Propagation
Volume 2012, Article ID 243191, 10 pages
doi:10.1155/2012/243191

Research Article

Effect of Earth Ground and Environment on Body-Centric Communications in the MHz Band

Katsuyuki Fujii and Yasuyuki Okumura

Faculty of Information Sciences and Engineering, Nanzan University, 27 Seirei-cho, Aichi, Seto 489-0863, Japan

Correspondence should be addressed to Katsuyuki Fujii, fujii@sd.nanzan-u.ac.jp

Received 27 February 2012; Revised 9 August 2012; Accepted 14 August 2012

Academic Editor: Deepti Das Krishna

Body area network (BAN) research, which uses the human body as a transmission channel, has recently attracted considerable attention globally. Zimmerman first advocated the idea in 1995. Illustrations of the electric field streamlines around the human body and wearable devices with electrodes were drawn. In the pictures, the electrodes of the wearable devices constitute a closed circuit with the human body and the earth ground. However, analysis of the circuit has not been conducted. In this study, we model the human body shunted to earth ground in a radio anechoic chamber to analyze the electric field strength around it and clarify the effect of earth ground during BAN run time. The results suggest that earth ground has little influence on the human body and wearable devices. Only when the human body is directly grounded, the electric field near the feet area will decrease. The input impedance of the transmitter is approximately the same, and the received open-circuit voltage and current of the receiver are also the same. In addition, we elucidate that stable communications can be established by developing a closed circuit using earth ground as return path. When the external electronic devices and human body are shunted to earth ground, the received open-circuit voltage and current increase.

1. Introduction

Research in wearable computing, which can always exchange information anywhere, has been actively pursued in recent years. For example, Zimmerman advocated the use of the human body as a transmission path [1, 2]. When a user wearing a transmitter with an electrode touches a receiver, a personal area network (PAN), which consists of the human body as the transmission path, is built. By transforming the human body into a transmission channel, transmission lines and communication need not occur during our daily activities. Moreover, it is unnecessary to establish a line of sight such as an IrDA, and energy consumption may be lower than that needed for wireless communications. Research on wearable devices is being performed by various organizations all over the world, and the expectations for utilization are growing. For example, the first technical textbook about BAN was published by Hall and Hao in 2006 [3]. Moreover, the second edition, which includes the latest research trends, was published in May 2012 [4]. In 2007, a task group for wireless personal area network (WPAN) was organized by IEEE [5], and, in 2009, the first special issue regarding this research field was published by IEEE [6]. In Japan, medical information and communications technology (MICT) is an active field [7]. In addition, medical applications that can receive health-monitoring information of humans are becoming important in an aging society.

The WPAN carrier frequency is different for each application. It is divided into two domains: (1) antenna propagation [10–12] and (2) electrostatic coupling [1, 2]. We have modeled the wearable devices attached to the human body as shown in Figure 1 and studied the transmission mechanisms of wearable devices using the human body as the transmission channel from the viewpoint of the interaction between the body and electromagnetic fields [8]. Furthermore, although the model analysis using the whole body has been conducted, the difference in the transmission characteristics which depends on the coupling between the human body and the earth ground has been unsolved. In near future, with the spread of wearable devices for WPAN,

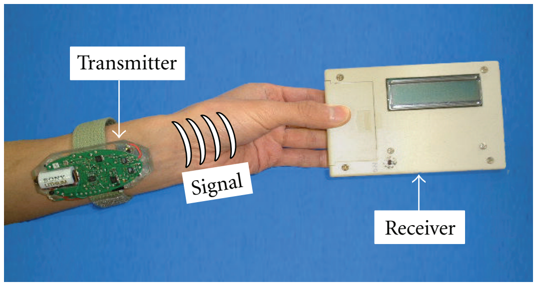

Figure 1: Transmission system using the human body as a transmission channel [8].

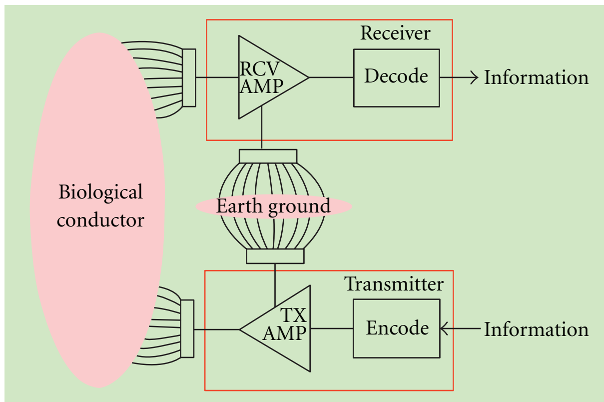

Figure 2: Electric field stream line model of PAN [1, 2].

wearable devices may be found almost everywhere on the human body, and they will exchange the data. To acquire a design guide in that case, it is necessary to understand how a signal is distributed over the whole body and how transmission characteristics change as a function of the environment.

2. Earth Ground and Transmission Characteristics

2.1. Analysis Model. In Zimmerman's studies [1, 2], there is coupling between earth ground and a biological conductor, as shown in Figure 2. However, few physical mechanisms that focus on ground have been explored until recently [9]. In this section, we model the human body with wearable devices in contact with earth ground in a radio anechoic chamber and report the effect of earth ground. Figure 3 shows the standard-posture model that has been simplified by dividing the body into legs, body, arms, shoulders, and head. Then, each part is modeled as a rectangular parallelepiped [9]. At 10 MHz, relative permittivity ($\varepsilon_r = 170.73$) and conductivity ($\sigma = 0.62$ S/m) are equal to the human muscle [13]. The size of the simplified body model is adapted from Japanese male and female averages, obtained from the statistical data [14].

The radio anechoic chamber at Chiba University is $7230 \times 5730 \times 2930\,\text{mm}^3$ in size, and it has a 70 mm thick concrete base ($\varepsilon_r = 3.8$, $\sigma = 6.67 \times 10^{-6}$ S/m, [15]) [16]. The absorber in the chamber is disregarded because we used 10 MHz sinusoidal waves that are not absorbed by the absorber. Perfect electric conductor sheets cover the ceiling, walls, and base under the concrete.

Figure 4 shows the structure of the wearable transmitter and receiver. This transmitter consists of one signal electrode and one circuit board. The signal electrode outputs a sinusoidal wave ($3\,\text{V}_{\text{p-p}}$) of 10 MHz. To apply this transmitter to finite difference time domain (FDTD) method, the electrode and circuit board are modeled by using perfect electric conductor sheets, and the delta-gap voltage of the 10 MHz sinusoidal wave is fed between the signal electrode and the circuit board. The receiver has one receiving electrode and one circuit board. The received open-circuit voltage (OCV) is calculated from the electric field between the receiving electrode and circuit board. The grid spacing of the FDTD method is $\Delta x = \Delta y = \Delta z = 5$ mm.

Figure 5 shows the calculation model of the human body in contact with earth ground with wearable devices in the radio anechoic chamber. The human body is in center of the chamber, and a perfect electric conductor sheet of $3000 \times 3000\,\text{mm}^2$ in size is placed under the legs.

Figure 6 shows four patterns of the simplified human-body model by varying the contact with earth ground (perfect electric conductor sheet). Figure 6(a) shows the legs directly shunted to earth ground, Figure 6(b) simulates the case of wearing shoes with a 3 cm thick sole, Figure 6(c) shows the far distance from the legs to ground (40 cm), and Figure 6(d) is for the free space case, in which the human body is not coupled to the surroundings. By using these calculation models, electric field distribution, OCV,

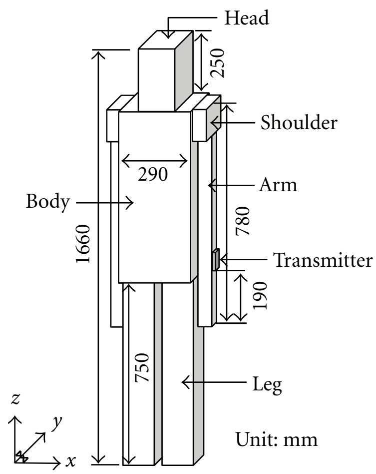

Figure 3: Simplified whole human body model [9].

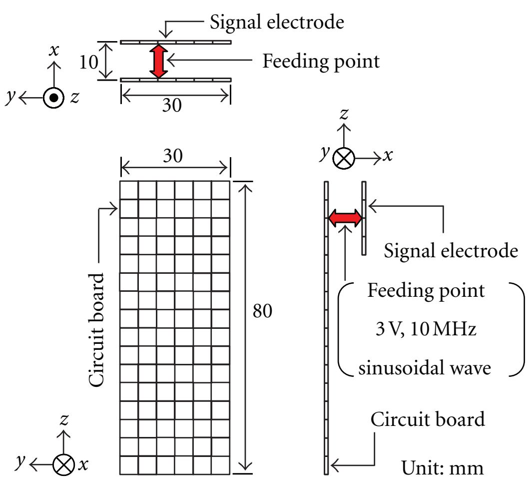

(a) FDTD calculation model of the wearable transmitter

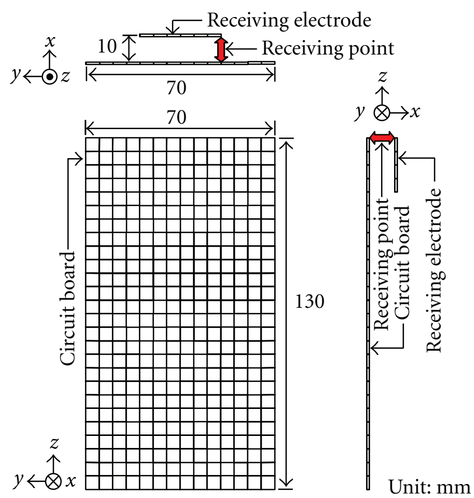

(b) FDTD calculation model of the wearable receiver

Figure 4: Structure of the wearable transmitter and receiver [8].

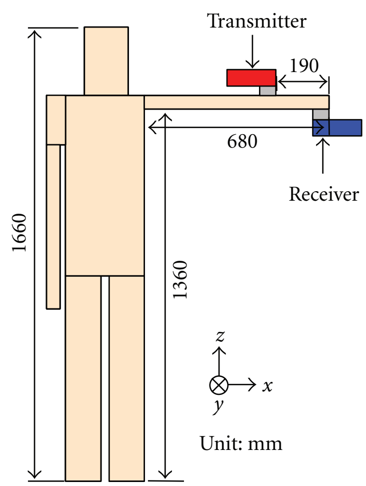

(a) Simplified human body with wearable devices

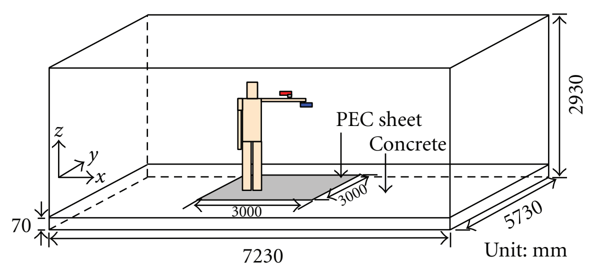

(b) Human body standing on the earth ground in the radio anechoic chamber

Figure 5: FDTD calculation model.

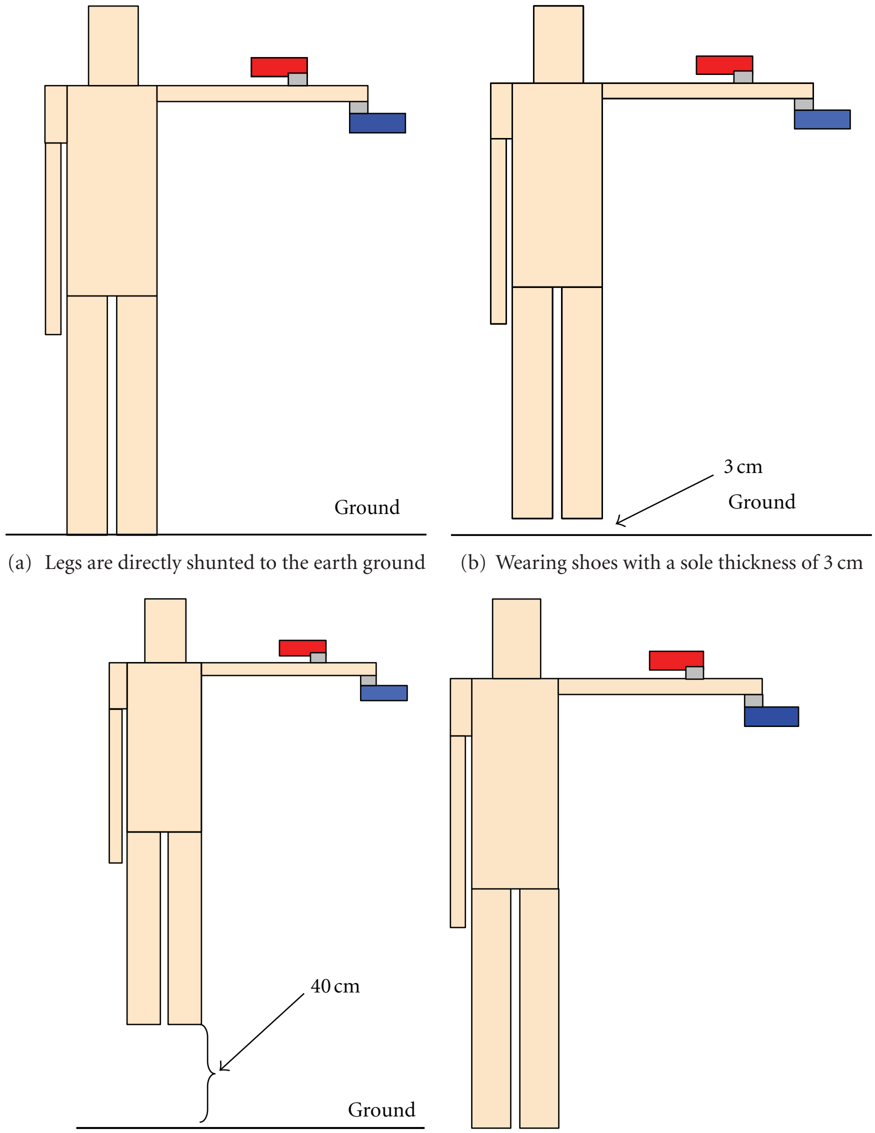

(a) Legs are directly shunted to the earth ground (b) Wearing shoes with a sole thickness of 3 cm

(c) Far distance from legs to ground (40 cm) (d) Human body in free space

Figure 6: Verification models for the influence of the earth ground.

Table 1: Input power and input impedance of the transmitter.

Model name	Input power (W)	Impedance (Ω)	
		Real	Imaginary
Ground	1.47×10^{-6}	20.9	−2825.6
3 cm up	1.43×10^{-6}	20.4	−2826.1
40 cm up	1.43×10^{-6}	20.2	−2826.2
Free space	1.43×10^{-6}	20.4	−2826.2

Table 2: OCV and current of the receiver.

Model name	OCV (mV)	J (nA)
Ground	9.19	72.1
3 cm up	9.26	73.1
40 cm up	9.48	74.4
Free space	9.55	75.1

and the receiver current are discussed considering the effect of earth ground in the radio anechoic chamber.

2.2. Calculation Results and Discussion. The results of the electric field distribution shown in Figures 7(a)–7(d) verify the influence of the earth ground. These figures illustrate the human body directly shunted to the earth ground, 3 cm above ground, 40 cm above ground, and in free space, respectively. It is evident that most of the electric field is distributed around the transmitter and along the arm. However, since the single-electrode structure of the transmitter was adopted, the radiation (leakage) in the air

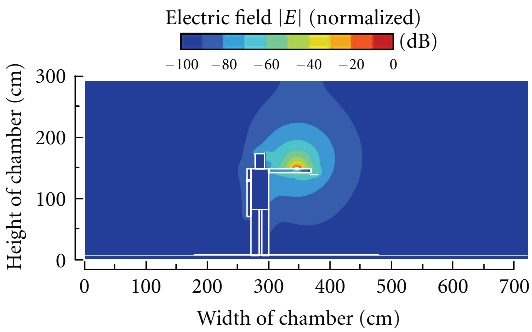

(a) Legs are directly shunted to the earth ground

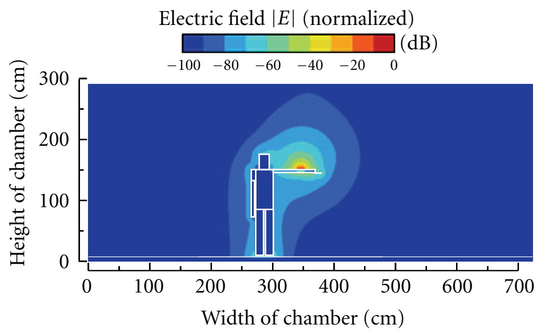

(b) 3 cm above the earth ground

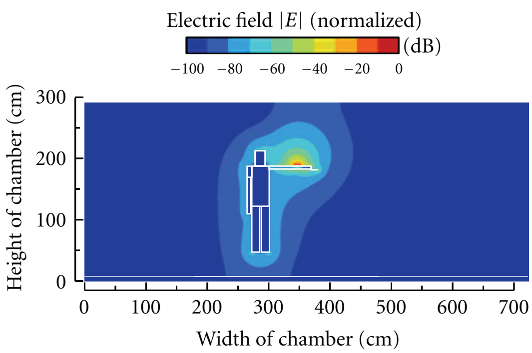

(c) 40 cm above the earth ground

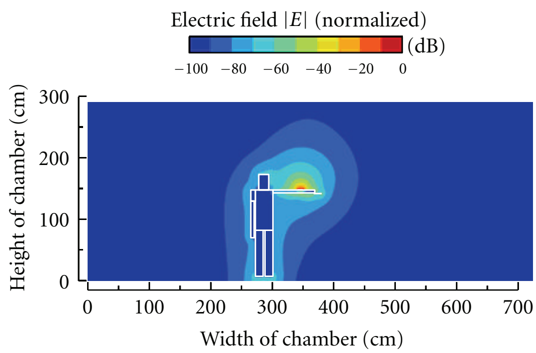

(d) Human body in free space

Figure 7: Electric field distribution around the human body.

Table 3: Input power and input impedance of the transmitter.

Model name	Input power (W)	Impedance (Ω)	
		Real	Imaginary
A. table w/leg	1.03×10^{-2}	53.5	−7.9
A. table w/o leg	1.02×10^{-2}	53.8	−7.7
w/o table	1.02×10^{-2}	53.9	−7.5
Free space	1.02×10^{-2}	53.9	−7.5
W. table w/leg	1.02×10^{-2}	53.9	−7.6
W. table w/o leg	1.02×10^{-2}	53.9	−7.6

Table 4: OCV and current of the receiver.

Model name	OCV (V)	J (μA)
A. table w/leg	0.63	4.92
A. table w/o leg	0.43	3.40
w/o table	0.27	2.13
Free space	0.26	2.03
W. table w/leg	0.31	2.44
W. table w/o leg	0.31	2.41

was strong. In Figure 7(a), the critical point is that the electric field strength decreases significantly around the leg region. It is assumed that existence of the earth ground prevents the electric field from the foot area. However, in the domain of the upper half of the body, there is no difference compared with other models. Moreover, from Figures 7(b) and 7(c), if the human body floats in the air, coverage of the electric field improves. These results show that when BAN devices are attached to the legs, the situation in which the legs are not directly shunted to the earth ground is effective.

Consideration for each vector component of the electric field is as follows. The electric field component perpendicular to the body surface is dominant. The human body acts as a conductor at 10 MHz because the loss tangent of the muscle is approximately 6.5. Therefore, while developing BAN devices, antennas designed to receive the perpendicular component of the electric field are required.

Table 1 shows input power and input impedance of the transmitter. It can be observed that input power is small because the one-electrode structure strengthens the capacitivity of the input impedance. However, even if the contact conditions with the earth ground change, the values of Table 1 remain constant. Table 2 shows the received OCV [mV] and current J [nA] of the receiver of each model. The strength remains constant because of the earth ground. From these results, it can be concluded that there is no coupling with earth ground. Therefore, only when the human body is directly grounded, the electric field near the feet area decreases.

3. Considering the Closed-Circuit Model through Earth Ground

3.1. Calculation Models. In this section, a closed-circuit model through earth ground is considered. This means hav-ing BAN communication with an external electronic device

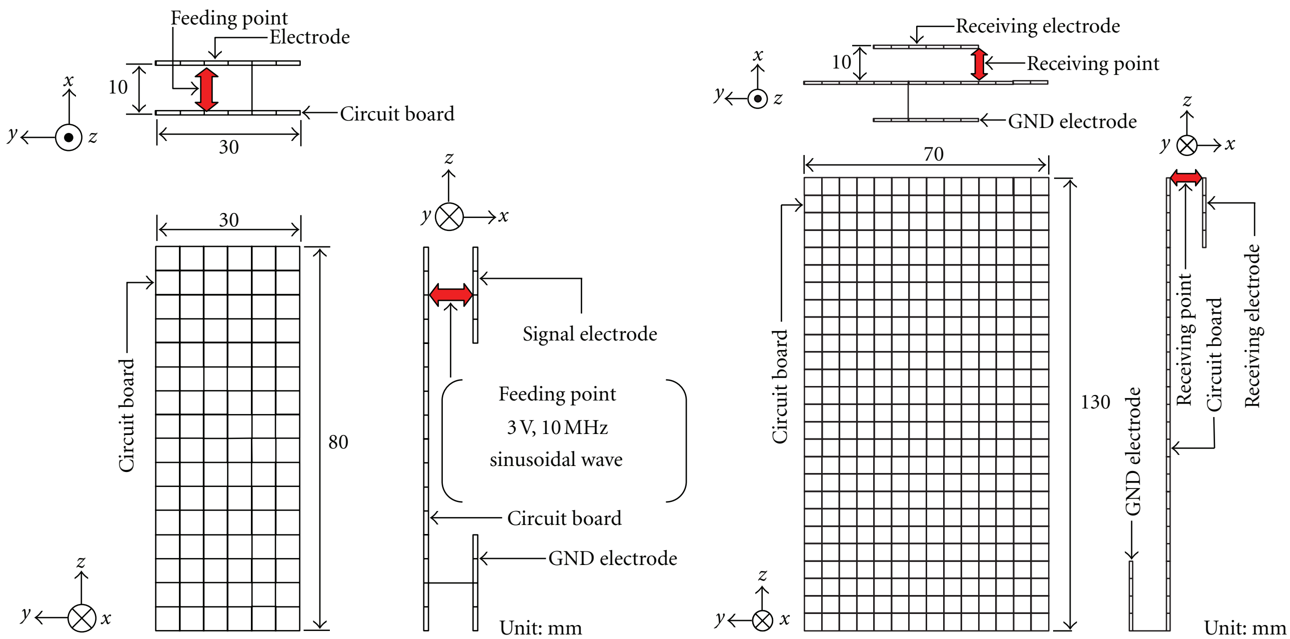

(a) FDTD calculation model of the transmitter

(b) FDTD calculation model of the receiver

Figure 8: FDTD calculation model of the transmitter and receiver.

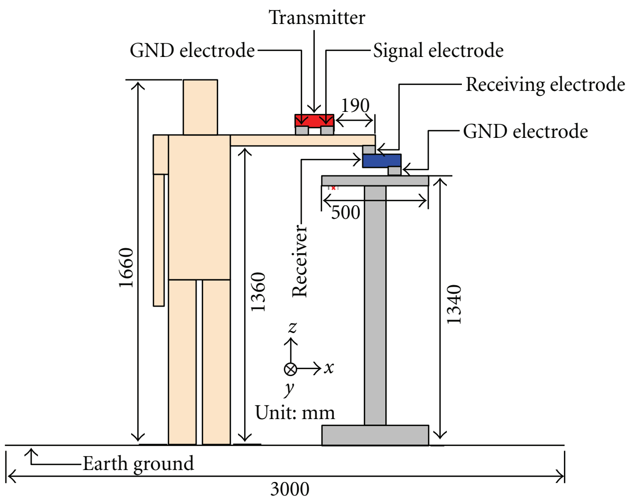

Figure 9: Calculation model of developing a closed circuit through the earth ground.

that is shunted to the stable earth ground level. Figure 8 shows FDTD calculation models of the wearable transmitter and receiver. The electrode structure is changed to establish a closed circuit through the earth ground. The transmitter has two electrodes [8]. One is a signal electrode, which feeds a 10 MHz sinusoidal wave ($3\,V_{p\text{-}p}$), and the other one is the ground (GND) electrode, which is shunted to the ground level of the transmitter. In addition, the receiver has two electrodes. One is the receiving electrode, and the other one is the GND electrode, which can be shunted to the earth ground.

Figure 9 shows the calculation model of developing the closed circuit through the earth ground. This figure is simply drawn so that the electrode structures, position, and environment are easily understood. The arm is lifted horizontally, similar to Section 2. The signal electrode is in contact at 190 mm from the fingertip. The receiving electrode is arranged under the fingertip. Moreover, to imitate an external device shunted to the earth ground, an aluminum table is modeled forming a current path to the earth ground.

In Figure 10, six types of situations are shown to clarify the effect of establishing a closed-circuit path through the earth ground. Each red line indicates the current path. In Figure 10(a), a tight circuit is formed by using an aluminum table ($\varepsilon_r = 1.00$, $\sigma = 3.82 \times 10^7$ S/m, [17]) shunted to the earth ground. Figure 10(b) shows the aluminum table without leg that interrupts the current path through the earth

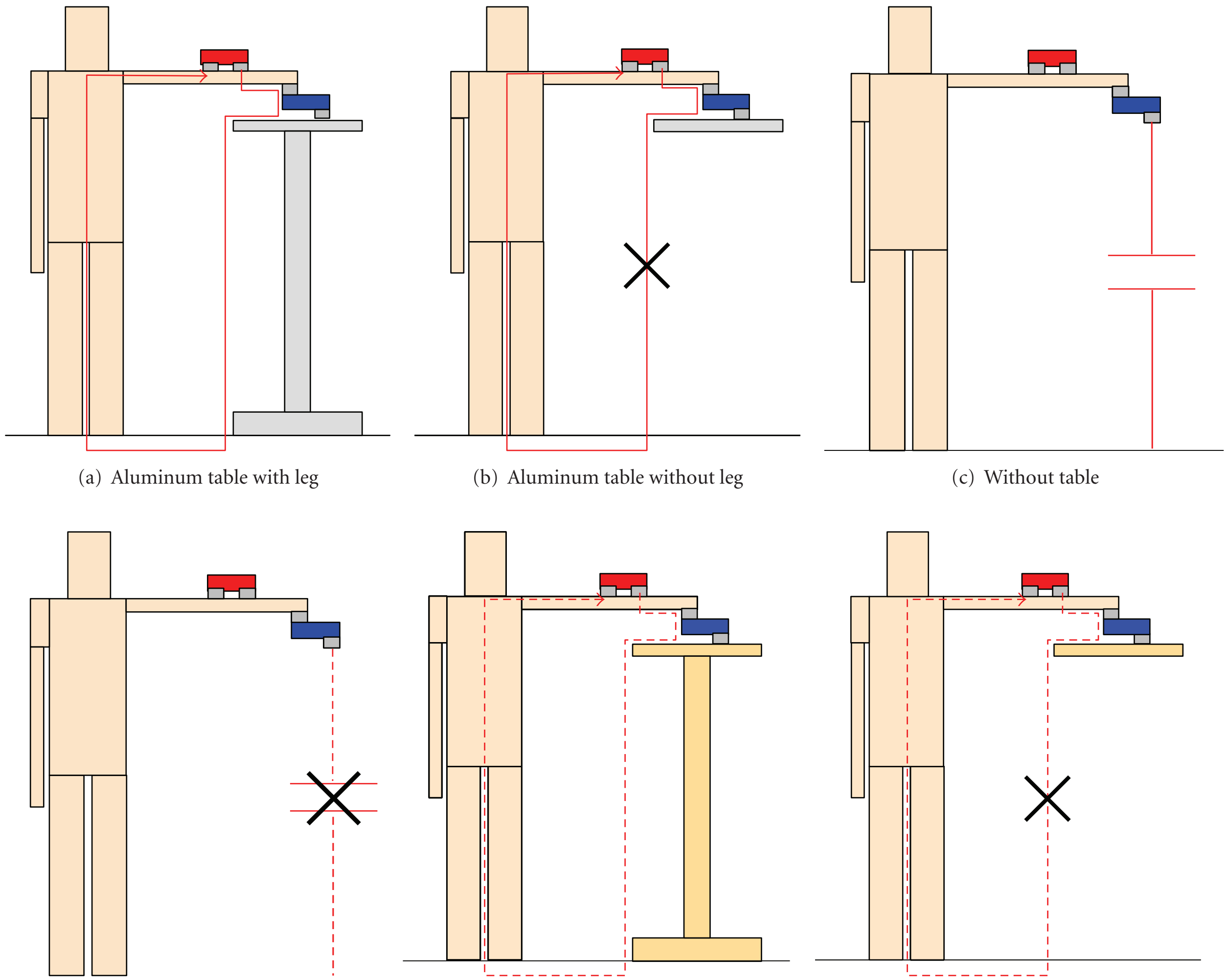

(a) Aluminum table with leg

(b) Aluminum table without leg

(c) Without table

(d) Free space

(e) Wooden table with leg

(f) Wooden table without leg

FIGURE 10: Analysis models for the effect of current loop path.

ground. Figure 10(c) shows the model that interrupts the circuit, so there is no influence of the surface of the aluminum table. Figure 10(d) shows the human body with wearable devices floating in free space. Therefore, the body is not influenced by the surroundings. Moreover, Figures 10(e) and 10(f) show the results of the analysis performed for a wooden table ($\varepsilon_r = 2.75$, $\sigma = 1.53 \times 10^{-5}$ S/m [17]) to clarify loose coupling.

3.2. Calculation Results and Discussion. In this section, we discuss the calculation results for the electric field strength, received OCV, and received current. All electric-field-strength data shown in Figure 11 are normalized to the electric field at the feeding gap. The electric field of each model is distributed along the human body. These tendencies are relatively similar to the results of Section 2. Besides, the input power and input impedance of the transmitter of each model in Table 3 are similar because GND electrode of the transmitter contributes to impedance matching [8]. Thus, the transmitter grounded to the human body is not influenced by the surroundings.

One of the notable features of electric field distribution is that the strength between the arms and the aluminum table with leg (shunted to the earth ground) is the greatest. The electric field concentration is due to the existence of large aluminum table with high conductivity and the return path of the current through the earth ground. This is the highest received OCV in Table 4. Furthermore, we can evaluate the validity of the closed-circuit model of Figure 2 by comparing the case between the aluminum table with legs and without legs.

The received OCV and current of the receiver in Table 4 suggest that it is advantageous to use the earth ground as a return path. When the return path is set, a stable connection can be constructed.

As a result, external BAN communication and wearable devices on the human body must share a stable earth ground connection to form the closed circuit, thereby allowing increased current flow to BAN area.

3.3. Measurement Results. In this section, we discuss the measurements of the received OCV from the receiver

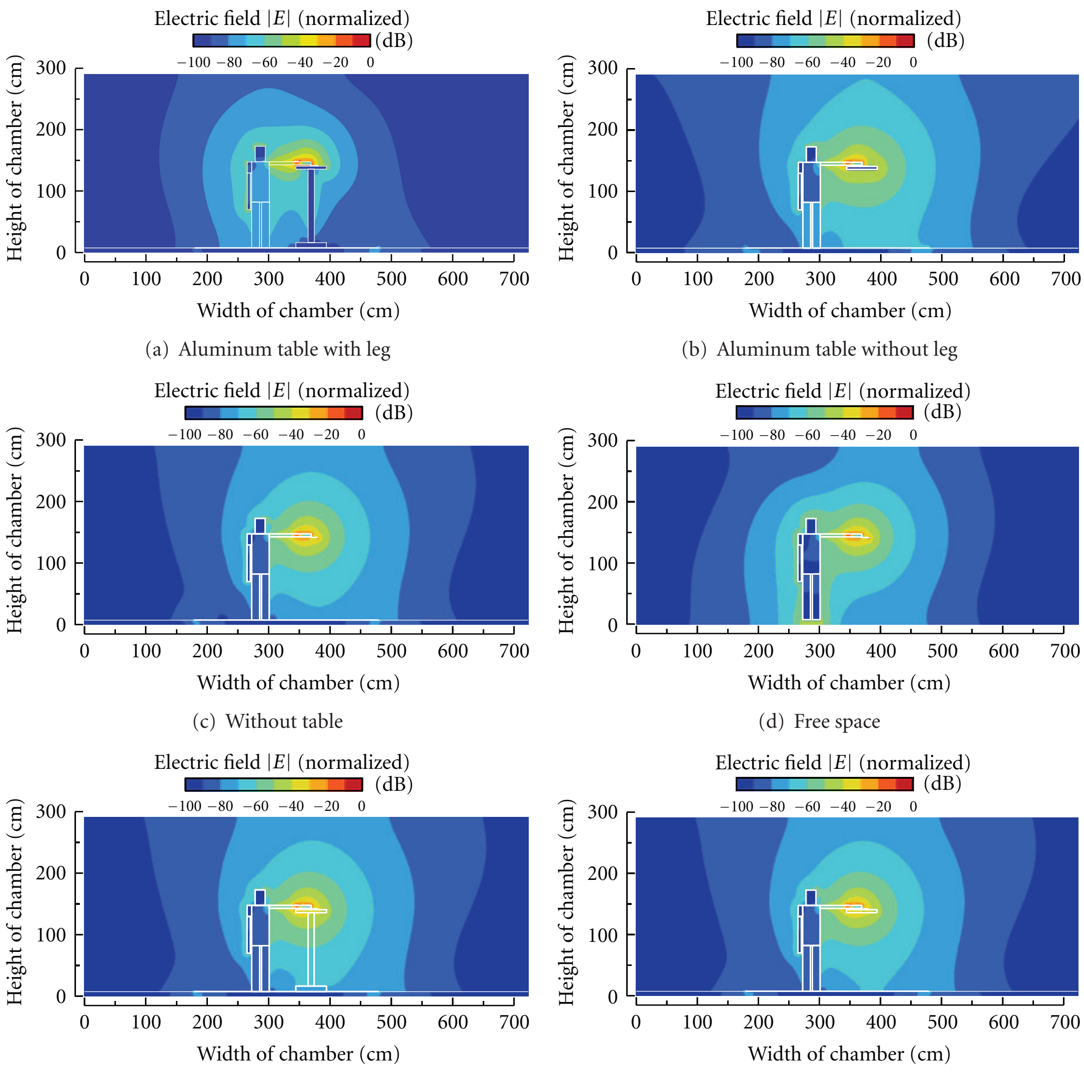

(a) Aluminum table with leg
(b) Aluminum table without leg
(c) Without table
(d) Free space
(e) Wooden table with leg
(f) Wooden table without leg

Figure 11: Electric field distribution.

to show the validity of the calculations. Figure 12 shows the measurement conditions. (Figure 12(a): aluminum table with leg, Figure 12(b): aluminum table without leg, Figure 12(c): without table, Figure 12(d): wooden table with leg, and Figure 12(e): wooden table without leg). The absorbers in the chamber are removed, and an aluminum plate, which imitates the earth ground, is set on the floor of the chamber with an area of $3000 \times 3000\,\text{mm}^2$. The electrode structures of the wearable transmitter and receiver are same as that of Figure 8. In the measurements, the feet of the human subject with the wearable devices are bare to directly shunt the body to the earth ground. The size of the subject is approximately the same as that of the calculation model based on the statistical data [14]. The measurement methods of reading the received OCV were severely restricted because the subject must maintain the same position during BAN run time. Thus, the measurements were obtained by another person that read the received OCV. In addition, the observer stood on styrene foam to avoid contact with the earth ground. Therefore, the voltage fluctuation due to the existence of the observer can be neglected.

Figure 13 shows the fluctuations in OCV in each environment. The values are normalized to the case of the "w/o table" model. As the diagram indicates, the measurements agree with the calculations. The results clearly show that the received OCV fluctuates between 96% and 233% as a function of the environment. When the closed circuit through the earth ground is constructed, the received OCV becomes stronger. Therefore, it is possibly reasonable to conclude that developing a closed circuit is advantageous for stable communication in BAN.

4. Conclusions

In this study, the effect of earth ground on transmission is analyzed by using a simplified model of the human body

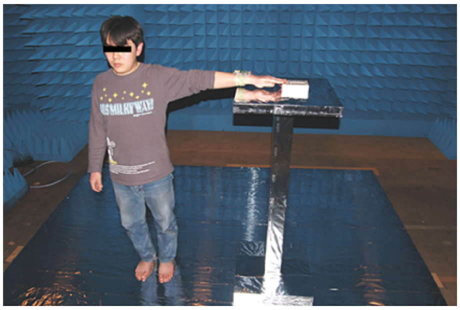

(a) Aluminum table with leg

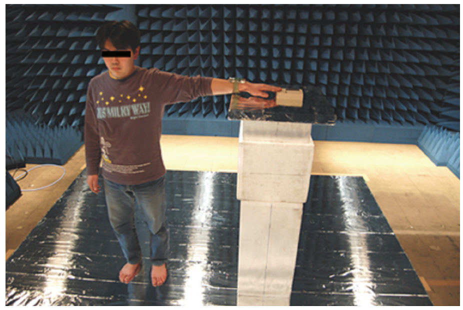

(b) Aluminum table without leg

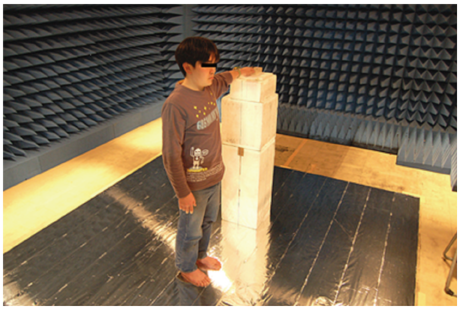

(c) Without table

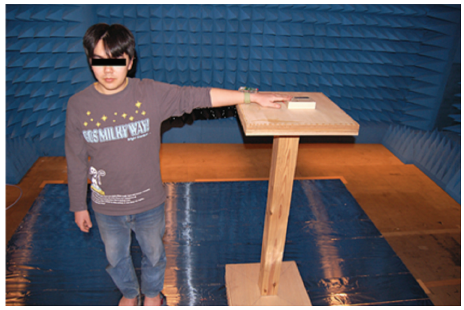

(d) Wooden table with leg

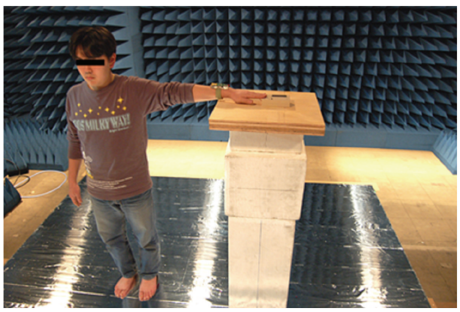

(e) Wooden table without leg

FIGURE 12: Measurement conditions.

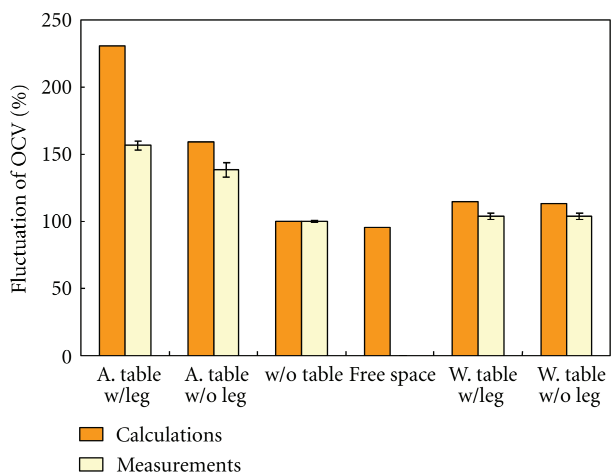

FIGURE 13: Fluctuations of OCV in each environment.

in contact with the earth ground with wearable devices in a radio anechoic chamber. The results are divided into two parts.

(1) The effect of earth ground on the wearable devices when there is no connection to ground.

(2) The effect on transmission when the human body, wearable devices, and the earth ground form a closed circuit.

In (1), four patterns of transmission were constructed. As a result, the input impedance of the transmitter is approximately the same, and the received OCV and current of the receiver at the fingertip are also the same. Thus, there is no effect on the signal of the transmission due to the earth ground coupling. Only when the human body is directly shunted to the earth ground, the electric field strength around the leg region weakens. In addition, when a human (whose body is considered) wears shoes (that means not directly shunted to the earth ground), electric field reduction cannot be observed, and this is approximately the same as that in the free space case.

In (2), when the external devices and human body are shunted to the earth ground (forming a closed circuit), the received OCV and current increase. This is because the current flow uses the earth ground to increase the closed circuit. Apparently, for a stable connection, it is advantageous to have the external devices and human body shunted to the earth ground. Moreover, the validity of the calculations is proved by the experiments in the radio anechoic chamber with a human.

Acknowledgments

The authors would specifically like to thank Professor Koichi Ito of Chiba University for his continuing guidance and encouragement and also wish to thank Associate Professors Masaharu Takahashi and Kazuyuki Saito of Chiba University for their valuable guidance. This study was partly supported by Nanzan University Pache Research Subsidy I-A-2 for the 2012 academic year.

References

[1] T. G. Zimmerman, *Personal Area Networks (PAN): near-field intra-body communication [M.S. thesis]*, MIT Media Laboratory, Cambridge, Mass, USA, 1995.

[2] T. G. Zimmerman, "Personal area networks: near-field intra-body communication," *IBM Systems Journal*, vol. 35, no. 3-4, pp. 609–617, 1996.

[3] P. S. Hall and Y. Hao, *Antennas and Propagation for Body-Centric Wireless Communications*, Artech House, 2006.

[4] P. S. Hall and Y. Hao, *Antennas and Propagation for Body-Centric Wireless Communications*, Artech House, 2nd edition, 2012.

[5] IEEE 802.15 WPAN Task Group 6, http://www.ieee802.org/15/pub/TG6.html.

[6] P. Hall, Y. Hao, and K. Ito, "Antennas and propagation on body-centric wireless communications," *IEEE Transactions on Antennas and Propagation*, vol. 57, no. 4, pp. 834–836, 2009.

[7] Technical Committee on Medical Information and Communication Technology (MICT), http://www.ieice.org/~mict/.

[8] K. Fujii, M. Takahashi, and K. Ito, "Electric field distributions of wearable devices using the human body as a transmission channel," *IEEE Transactions on Antennas and Propagation*, vol. 55, no. 7, pp. 2080–2087, 2007.

[9] K. Fujii, D. Ishide, M. Takahashi, and K. Ito, "Electric field distributions generated by a wearable device using simplified whole human body models," *Journal of the Institute of Image Information and Television Engineers*, vol. 62, no. 12, pp. 1980–1987, 2008.

[10] S. L. Cotton and W. G. Scanlon, "Channel characterization for single- and multiple-antenna wearable systems used for indoor body-to-body communications," *IEEE Transactions on Antennas and Propagation*, vol. 57, no. 4, pp. 980–990, 2009.

[11] I. Khan and P. S. Hall, "Multiple antenna reception at 5.8 and 10 GHz for body-centric wireless communication channels," *IEEE Transactions on Antennas and Propagation*, vol. 57, no. 1, pp. 248–255, 2009.

[12] P. Van Torre, L. Vallozzi, C. Hertleer, H. Rogier, M. Moeneclaey, and J. Verhaevert, "Indoor Off-Body wireless MIMO communication with dual polarized textile antennas," *IEEE Transactions on Antennas and Propagation*, vol. 59, no. 2, pp. 631–642, 2011.

[13] IFAC, http://niremf.ifac.cnr.it/tissprop/.

[14] Report of National Institute of Bioscience and Human-Technology, "Human body dimensions data for ergonomic design," vol. 2, no. 1, 1994.

[15] C. Cristina and A. Orlandi, "Equivalent transmission line model for electromagnetic penetration through reinforced concrete walls," *IEICE Transactions on Communications*, vol. 78, no. 2, pp. 218–229, 1995.

[16] K. Fujii, K. Ito, and S. Tajima, "A study on the signal propagation of whole body model wearing transmitter using human body as a transmission channel," in *Proceedings of the ITE annual convention*, Tokyo, Japan, August 2003.

[17] W. Hayt and J. Buck, *Engineering Electromagnetics*, McGraw-Hill, 2001.